

NOTE

JBIR-17, a novel trichostatin analog from *Streptomyces* sp. 26634

Jun-ya Ueda¹, Ji-Hwan Hwang², Satoko Maeda³, Taira Kato⁴, Atsushi Ochiai⁴, Kunio Isshiki⁴, Minoru Yoshida³, Motoki Takagi¹ and Kazuo Shin-ya²

The Journal of Antibiotics (2009) 62, 283–285; doi:10.1038/ja.2009.22; published online 20 March 2009

Keywords: histone deacetylase; histone deacetylase inhibitor; *Streptomyces*; trichostatin

Histone deacetylases (HDACs) play an important role in the epigenetic regulation of gene expression by catalyzing the removal of acetyl groups from lysine residue of histone protein, stimulating chromatin condensation and promoting transcriptional repression.^{1,2} HDACs are divided into four classes on the basis of their homology to yeast HDACs: class I (HDAC1, 2, 3 and 8), class IIa (HDAC4, 5, 7 and 9), class IIb (HDAC6 and 10), class III (SIRT1, 2, 3, 4, 5, 6 and 7) and class IV (HDAC11). As aberrant epigenetic changes are a hallmark of cancer, HDACs are a promising target for an anticancer drug. The inhibitors of HDACs can induce cell-cycle arrest, promote differentiation and stimulate tumor cell death. In fact, several HDAC inhibitors are currently in clinical trials both for solid and hematological malignancies.^{1,2} Therefore, we attempted to search new HDAC inhibitors. As a result, we isolated a novel compound designated as JBIR-17 (**1**) from *Streptomyces* sp. 26634 (Figure 1). We report herein the isolation, structure elucidation and biological activity of **1**.

Streptomyces sp. 26634 was isolated from a leaf of *Kerria japonica* collected in Iwata, Shizuoka Prefecture, Japan, and cultured on a rotary shaker (220 r.p.m.) at 28°C for 4 days in a 500-ml Erlenmeyer flask containing 60 ml of a medium consisting of 4% β -cyclodextrin, 0.5% glycerol, 2% Pharmamedia (Traders Protein, Lubbock, TX, USA), 0.0005% $\text{CuSO}_4 \cdot 5\text{H}_2\text{O}$, 0.0005% $\text{MnCl}_2 \cdot 4\text{H}_2\text{O}$ and 0.0005% $\text{ZnSO}_4 \cdot 7\text{H}_2\text{O}$.

n-BuOH (37.5 ml) was added to the fermentation broth (60 ml) and shaken for 15 min. After centrifugation, the organic layer was evaporated *in vacuo*. The dried residue (107 mg) was subjected to reversed-phase medium-pressure liquid chromatography (Purif-Pack ODS 100, Moritex, Tokyo, Japan) and eluted with a MeOH–H₂O (5–100% MeOH) linear gradient system. The 70–90% MeOH eluate (3.7 mg) was further purified by reversed-phase HPLC using an

XBridge Prep C₁₈ column (5 μm optimum bed density (OBD), 4.6 i.d. \times 250 mm, Waters, Milford, MA, USA) with 35% aqueous CH₃CN containing 0.2% formic acid (flow rate, 1 ml min⁻¹) to yield JBIR-17 (**1**, 0.9 mg; retention time (Rt) 9.7 min) and trichostatin A (**2**, 0.7 mg; Rt 10.3 min).³

The physicochemical properties of **1** are summarized in Table 1. Compound **1** was obtained as a colorless amorphous solid, and its molecular formula was determined to be C₂₀H₂₆N₂O₅ by HR-electrospray ionization (ESI)-MS. The IR spectrum revealed the characteristic absorptions of the aroyl and/or amide carbonyl (ν_{max} 1652 cm⁻¹) and amide N-H (ν_{max} 1597 cm⁻¹) groups. The structure of **1** was mainly determined by NMR spectral analyses as follows.

The direct connectivity between each proton and carbon was established by the heteronuclear single quantum coherence spectrum, and the ¹³C and ¹H NMR spectral data for **1** are shown in Table 2. A total of 20 signals were observed in the ¹³C NMR spectrum, consistent with the HR-MS data. These signals included three carbonyl (C-1, C-7, C-1'), four olefinic (C-2 to C-5) and six aromatic (C-8 to C-13) carbons. The proton spin couplings between two olefinic protons 2-H (δ_{H} 5.91) and 3-H (δ_{H} 7.28), between an olefinic proton 5-H (δ_{H} 6.04) and a methyl proton 6-Me (δ_{H} 1.28) through a methine proton 6-H (δ_{H} 4.36), and between two equivalent aromatic protons 9,13-H (δ_{H} 7.84) and 10,12-H (δ_{H} 6.69) on a *p*-disubstituted benzene ring were observed in a double-quantum filtered (DQF)-COSY spectrum as shown in Figure 2 (bold line). The constant time heteronuclear multibond correlation (CT-HMBC) experiment revealed the presence of ¹H–¹³C long-range couplings from an *N,N*-dimethyl proton (δ_{H} 3.05) to an aromatic carbon C-11 (δ_{C} 155.2), from 9,13-H to C-11 and a carbonyl carbon C-7 (δ_{C} 198.7), from 10,12-H to an aromatic carbon C-8 (δ_{C} 127.0), from 6-Me, 6-H and 5-H to C-7, from the

¹Biomedical Information Research Center (BIRC), Japan Biological Informatics Consortium (JBIC), Koto-ku, Tokyo, Japan; ²Biomedical Information Research Center (BIRC), National Institute of Advanced Industrial Science and Technology (AIST), Koto-ku, Tokyo, Japan; ³Chemical Genomics Research Group/Chemical Genetics Laboratory, RIKEN Advanced Science Institute, Wako, Saitama, Japan and ⁴Bioresource Laboratories, Mercian Corporation, Iwata, Shizuoka, Japan

Correspondence: Dr M Takagi, Biomedical Information Research Center (BIRC), Japan Biological Informatics Consortium (JBIC), 2-42 Aomi, Koto-ku, Tokyo 135-0064, Japan. E-mail: motoki-takagi@aist.go.jp or

Dr K Shin-ya, Biomedical Information Research Center (BIRC), National Institute of Advanced Industrial Science and Technology (AIST), 2-42 Aomi, Koto-ku, Tokyo 135-0064, Japan.

E-mail: k-shinya@aist.go.jp

Received 4 February 2009; revised 26 February 2009; accepted 27 February 2009; published online 20 March 2009

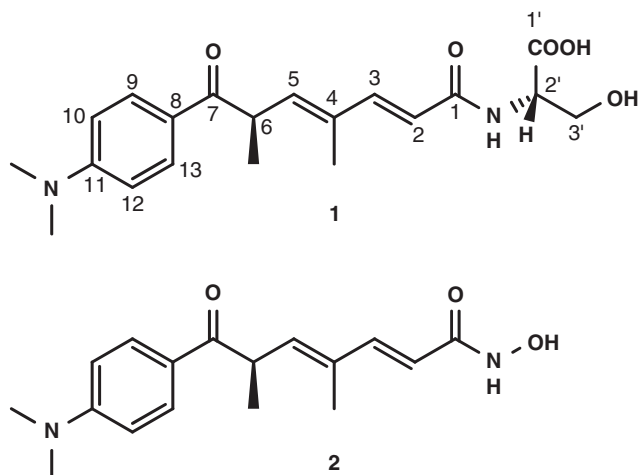


Figure 1 Structures of JBIR-17 (**1**) and trichostatin A (**2**).

Table 1 Physicochemical properties of **1**

Appearance	Colorless amorphous solid
Optical rotation ^a	$[\alpha]_D^{25} -18.0^\circ$ (c 0.1, MeOH)
HR-ESI-MS ^b (m/z)	
Found	375.1880 (M+H) ⁺
Calculated	375.1920 (C ₂₀ H ₂₇ N ₂ O ₅)
UV ^c λ_{max} nm (ϵ)	264 (24 700), 336 (23 500)
IR ^d (KBr) ν_{max} cm ⁻¹	3415, 1653, 1597

Abbreviation: ESI, electrospray ionization.

^aOptical rotation was measured on a SEPA-300 polarimeter (Horiba, Kyoto, Japan).

^bHR-ESI-MS measurement was carried out on a LCT Premier XE mass spectrometer (Waters).

^cUV spectrum was measured on a COULTER DU730 UV/Vis Spectrophotometer (Beckman, Fullerton, CA, USA).

^dIR spectra was obtained on a FT-720 Fourier transform infrared spectrometer (Horiba).

Table 2 ¹³C and ¹H NMR data for **1**

Position	δ_C	δ_H
1	168.6	
2	117.5	5.91 (d, 15.4)
3	147.5	7.28 (d, 15.4)
4	132.5	
5	141.9	6.04 (d, 9.5)
6	40.9	4.36 (dq, 9.5, 6.9)
7	198.7	
8	127.0	
9, 13	130.7	7.84 (d, 8.8)
10, 12	111.2	6.69 (d, 8.8)
11	155.2	
1'	172.0	
2'	54.8	4.60 (br s)
3'	62.1	4.18 (br d, 10.5); 3.85 (br d, 10.5)
4-methyl	12.6	1.89 (s)
6-methyl	17.8	1.28 (d, 6.9)
11 N,N-dimethyl	40.3	3.05 (s)

¹³C (125 MHz) and ¹H (500 MHz) NMR spectra were taken on a NMR System 500 NB CL (Varian, Palo Alto, CA, USA) in CDCl₃, and the solvent peak was used as an internal standard (δ_C 77.0, δ_H 7.26).

vinyl methyl proton 4-Me (δ_H 1.89) to three olefinic carbons C-3 (δ_C 147.5), C-4 (δ_C 132.5) and C-5 (δ_C 141.9), and from 2-H and 3-H to an amide carbonyl carbon C-1 (δ_C 168.6). The stereochemistries of



Figure 2 Key correlations in DQF-COSY (bold line) and CT-HMBC (arrow) spectra of **1**.

two olefins were determined as 2*E* and 4*E* according to the coupling constant ($J_{2,3}=15.4$ Hz) and the high-field-shifted ¹³C chemical shift at 4-Me (δ_C 12.6). Thus, the partial structure was elucidated as a trichostatin acid (**3**) moiety, and their ¹³C and ¹H NMR signals are superimposable with those of **2**³ and **3**⁴.

Additional substructure was elucidated as follows. A proton spin coupling between an α -methine proton 2'-H (δ_H 4.60; δ_C 54.8) and oxymethylene protons 3'-H (δ_H 4.18, 3.85; δ_C 62.1) was observed. A long-range coupling from 3'-H to a carboxylic carbonyl carbon C-1' deduced that the remaining structure was a serine moiety, and the serine was assumed to attach to C-1 of trichostatin through an amide bond.

The linkage position and the absolute configuration of the serine moiety of **1** were confirmed as follows. To determine the absolute configuration of the serine moiety, Marfey's method was adopted. Compound **1** (0.8 mg) was hydrolyzed with 6 N HCl (0.2 ml) at 120°C overnight to obtain the serine residue. After acid hydrolysis, the reaction solution was adjusted to neutral pH and evaporated *in vacuo*. The residue was dissolved in an aqueous solution of 0.1 M NaHCO₃ (0.6 ml), and 10 mM *N*^α-(5-fluoro-2,4-dinitrophenyl)-L-alaninamide (FDAA) in Me₂CO (0.6 ml) was successively added. The mixture was kept at 70°C for 10 min with frequent shaking. After work-up with the addition of 0.2 N HCl, the filtered reaction mixture was subjected to ultra performance liquid chromatography (UPLC) analysis (Acquity UPLC BEH C₁₈ 1.7 μ m, 2.1 \times 50 mm, Waters; 10% aqueous CH₃CN containing 0.1% formic acid; flow rate, 0.3 ml min⁻¹). The authentic D- and L-serine were reacted with FDAA in the same manner as described above. The serine residue obtained from the hydrolysate was determined to be L-serine (Rt 8.6 min; L-Ser, 8.5 min; D-Ser, 9.8 min). To confirm the linkage position of serine moiety, **1** was semi-synthesized from **2** as shown in Figure 3. Briefly, **2** (7.5 mg) was converted to **3** (3.4 mg) by HClO₄. Compound **3** was coupled with an *O*-*t*-butyl-L-serine *t*-butyl ester in the presence of PyBOP and *N,N*-diisopropylethylamine followed by deprotection in acidic condition to yield an L-serine adduct of **3** (0.9 mg). This synthetic compound showed an identical ¹H NMR spectrum to that of naturally isolated **1** from *Streptomyces* sp. 26634.

To evaluate inhibitory activity for HDACs of **1**, we used the reporter gene assay system using a luciferase gene as described earlier.^{5,6} The human embryonic kidney 293T cells, transformed with the luciferase reporter gene driven by the cytomegalovirus promoter, produced 2.5 times more luciferase compared with the untreated control, when they were treated with **1** at a concentration of 30 μ M. Furthermore, to clarify the selectivity against HDAC subtypes, **1** was tested in the HDAC inhibitory activity using HDAC1 (class I), 4 (class IIa) and 6 (class IIb) enzymes of 293T cell origin, which are usually used as the representative HDACs among each HDAC subtype.⁷ Compound **1** showed inhibitory activity against HDAC4 and 6 with IC₅₀ values of 69 and 4.7 μ M, respectively, but no activity against HDAC1 at a

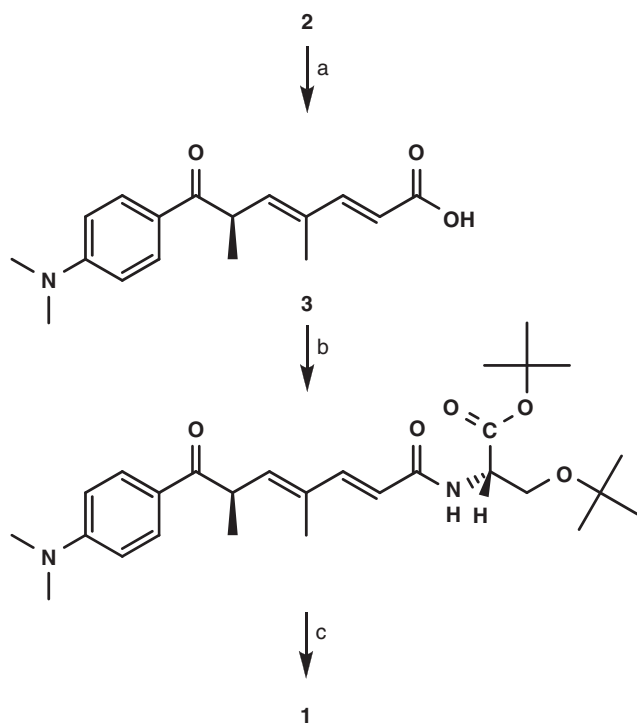


Figure 3 Scheme of chemical conversion from **2** to **1**. (a) 1.5 N HClO₄ aq, 50°C, overnight. (b) *O*-*t*-butyl-L-serine *t*-butyl ester, PyBOP, *N,N*-diisopropylethylamine in CH₂Cl₂/DMF (*N,N*-dimethylformamide), room temperature, 2 h. (c) 90% aqueous trifluoroacetic acid, room temperature, 1.5 h.

concentration of 100 μM. In contrast, **2** showed strong, but not selective, inhibitory effects against these HDACs (IC₅₀ values, 18, 30 and 92 nM against HDAC1, 4 and 6, respectively) as reported earlier.^{8,9} These results indicated that **1** selectively inhibited HDAC6 compared with HDAC1 and 4. HDAC6 is a cytoplasmic enzyme that regulates many important biological processes, including cell migration, immune synapse formation, viral infection and the degradation of

misfolded proteins. Furthermore, HDAC6 deacetylates tubulin, Hsp90 and cortactin.^{10–12} The diverse functions of HDAC6 suggest that it is a potential therapeutic target for a wide range of diseases. Thus, JBIR-17 could be a valuable tool for the studies of HDAC6 and enzymatic property among HDAC subtypes.

ACKNOWLEDGEMENTS

This work was supported in part by the New Energy and Industrial Technology Development Organization of Japan (NEDO), and a Grant-in-Aid for Scientific Research (20380070 to KS) from the Japan Society for the Promotion of Science (JSPS).

- 1 Carew, J. S., Giles, F. J. & Nawrocki, S. T. Histone deacetylase inhibitors: mechanisms of cell death and promise in combination cancer therapy. *Cancer Lett.* **269**, 7–17 (2008).
- 2 Shankar, S. & Srivastava, R. K. Histone deacetylase inhibitors: mechanisms and clinical significance in cancer: HDAC inhibitor-induced apoptosis. *Adv. Exp. Med. Biol.* **615**, 261–298 (2008).
- 3 Tsuji, N., Kobayashi, M., Nagashima, K., Wakisaka, Y. & Koizumi, K. A new antifungal antibiotic, trichostatin. *J. Antibiot.* **29**, 1–6 (1976).
- 4 Tsuji, N. & Kobayashi, M. Trichostatin C, a glucopyranosyl hydroxamate. *J. Antibiot.* **31**, 939–944 (1978).
- 5 Numajiri, Y., Takahashi, T., Takagi, M., Shin-ya, K. & Doi, T. Total synthesis of largazole and its biological evaluation. *Synlett.* **16**, 2483–2486 (2008).
- 6 Dressel, U., Renkawitz, R. & Baniahmad, A. Promoter specific sensitivity to inhibition of histone deacetylases: implications for hormonal gene control, cellular differentiation and cancer. *Anticancer Res.* **20**, 1017–1022 (2000).
- 7 Shivashimpi, G. M. *et al.* Molecular design of histone deacetylase inhibitors by aromatic ring shifting in chlamydocin framework. *Bioorg. Med. Chem.* **15**, 7830–7839 (2007).
- 8 Yoshida, M., Kijima, M., Akita, M. & Beppu, T. Potent and specific inhibition of mammalian histone deacetylase both *in vivo* and *in vitro* by trichostatin A. *J. Biol. Chem.* **265**, 17174–17179 (1990).
- 9 Furumai, R., Komatsu, Y., Nishino, N., Khochbin, S., Yoshida, M. & Horinouchi, S. Potent histone deacetylase inhibitors built from trichostatin A and cyclic tetrapeptide antibiotics including trapoxin. *Proc. Natl Acad. Sci. USA* **98**, 87–92 (2001).
- 10 Valenzuela-Fernández, A., Cabrero, J. R., Serrador, J. M. & Sánchez-Madrid, F. HDAC6: a key regulator of cytoskeleton, cell migration and cell-cell interactions. *Trends Cell Biol.* **18**, 291–297 (2008).
- 11 Rodríguez-Gonzalez, A. *et al.* Role of the aggresome pathway in cancer: targeting histone deacetylase 6-dependent protein degradation. *Cancer Res.* **68**, 2557–2560 (2008).
- 12 Matthias, P., Yoshida, M. & Khochbin, S. HDAC6 a new cellular stress surveillance factor. *Cell Cycle* **7**, 7–10 (2008).